

LIMNOLOGY AND OCEANOGRAPHY

March 2001

Volume 46

Number 2

Limnol. Oceanogr., 46(2), 2001, 213–223
© 2001, by the American Society of Limnology and Oceanography, Inc.

Remote sensing of biotic effects: Zebra mussels (*Dreissena polymorpha*) influence on water clarity in Saginaw Bay, Lake Huron

Judith W. Budd

Department of Geological Engineering and Sciences, Michigan Technological University, 1400 Townsend Drive, Houghton, Michigan 49931

Thomas D. Drummer

Department of Mathematical Sciences, Michigan Technological University, 1400 Townsend Drive, Houghton, Michigan 49931

Thomas F. Nalepa

NOAA/Great Lakes Environmental Research Laboratory, 2205 Commonwealth Boulevard, Ann Arbor, Michigan 48105

Gary L. Fahnenstiel

NOAA/Great Lakes Environmental Research Laboratory, Lake Michigan Field Station, 1431 Beach Street, Muskegon, Michigan 49441

Abstract

In this study, Advanced Very High Resolution Radiometer (AVHRR) remote sensing reflectance (R_{rs}), imagery from 1987–1993 is used to study changes in water clarity before and after zebra mussels (*Dreissena polymorpha*) were discovered in Saginaw Bay, Lake Huron. Spatial and temporal trends in the data indicate distinct and persistent increases in water clarity in the inner bay after the first large recruitment of zebra mussels in the fall of 1991. The pre-*Dreissena* imagery show that turbidity in the inner bay was influenced by the Saginaw River discharge in spring, biological production (plankton) in summer, and wind-driven resuspension in fall, with highest turbidity in spring and fall. Spatial patterns in the post-*Dreissena* images were more similar regardless of season, with low reflectances in the shallow regions of the inner bay where zebra mussel densities were highest. A regression model based on point data from 24 sampling stations over the 7-yr period indicates that reflectances varied significantly by site and zebra mussel densities, as well as seasonally. Trends in observed and predicted values of reflectances followed similar patterns at each station—highest values were found during 1991 and lowest during 1992 at all stations, with slightly higher R_{rs} in 1993 compared to 1992. Whereas AVHRR R_{rs} highlight the value of historical imagery for reconstructing seasonal and interannual turbidity patterns in near-shore waters, a new generation of operational ocean color satellites, such as SeaWiFS (Sea-viewing Wide Field-of-view Sensor) and the newly launched MODIS (moderate resolution imaging spectroradiometer), now provide for routine monitoring of important biological and physical processes from space.

Saginaw Bay, Lake Huron was one of the last major bays in the Great Lakes to be colonized by zebra mussels (*Dreis-*

sena polymorpha). Ecosystem-level studies of zebra mussel effects were initiated in 1990, immediately prior to zebra mussel colonization, and continued until 1993 when zebra mussels were firmly established in the bay (Nalepa and Fahnenstiel 1995). Although zebra mussels were found in Saginaw Bay in 1990, the first large recruitment of post-veliger larvae did not occur until August 1991 (Nalepa et al. 1995). Adult zebra mussel densities ranged from 4,000 to 57,000 at high-density sites and 0 to 3,000 at low-density sites in 1992 and 1993. The filtration capacity of the mussel population was 1.3 and 0.2 times the volume of the inner bay per day, respectively, for these years (Fanslow et al. 1995). Water quality changes were apparent in Saginaw Bay as early as the fall of 1991 (Fahnenstiel et al. 1995). Trends followed

Acknowledgments

We thank W. Charles Kerfoot, Richard P. Stumpf, and two anonymous reviewers for critical comments on the manuscript.

This research was supported by grants from the Office of Sea Grant (SG-1993-08), through the Cooperative Institute for Limnology and Ecosystems Research (CILER), Michigan Sea Grant College Program Fund RA0547-MICHI.; and the National Aeronautics and Space Administration (Grant NRA 94-PSS-16). This paper is NOAA/GLERL Contribution No. 1173. State of Michigan Research Excellence Funds, provided by the MTU Lake Superior Ecosystem Research Center (LaSER), supported the purchase of computer hardware and imaging processing software.

the same patterns as in other Great Lakes near-shore regions, including significantly lower total suspended solids and chlorophyll *a* (Chl *a*) concentrations and increased Secchi disc visibilities (Fahnenstiel et al. 1995; Johengen et al. 1995).

Associated ecosystem changes, such as increased water clarity and decreased Chl *a* levels, have fundamentally changed the optical characteristics of Great Lakes basins and embayments. Whereas water quality studies rely on point data from shipboard sampling, laboratory experiments, and enclosures, the scale and magnitude of zebra mussel effects suggest an additional research application that involves satellite remote sensing technology. Satellite image analysis complements shipboard sampling efforts by providing frequent overflights and synoptic reconnaissance of surface waters. Furthermore, archives of remotely sensed data facilitate retrospective analyses of water quality conditions in the Great Lakes during periods when in situ water quality data are not available. Here we test the feasibility of using remote sensing data from the advanced very high resolution radiometer (AVHRR) to determine ecosystem impacts.

The ability of AVHRR imagery to resolve temperature differences is well documented (Budd et al. 1998, 1999; Leshkevich et al. 1993; McMillan and Crosby 1984). Less appreciated is the fact that AVHRR also has the sensitivity and dynamic range to provide usable data on suspended sediments for estuaries and embayments, provided there is a wide range in turbidity at the particular site. Stumpf (1995) and Stumpf and Frayer (1997), in particular, have advocated application of AVHRR red and near infrared channels to this problem. Stumpf used vector analyses to relate water color to remote sensing reflectance (R_{rs}) to calculate suspended particle concentrations. In his studies of Chesapeake Bay, he found satellite measurement of sediment concentration was as accurate as $\pm 30\%$ (Stumpf and Tyler 1988).

Seasonal and interannual variation in suspended solids in near-shore regions is an important factor in evaluating changes in water quality; however, great spatial and temporal variability exists. In this investigation, we examined the variability in surface suspended solids using satellite measurements to determine the degree to which these features change seasonally, interannually, and due to zebra mussel occurrence; the impact of other near-shore phenomena (e.g., river plumes, sediment resuspension, exchange with Lake Huron near-shore waters) on the detection of zebra mussel effects; and the extent to which physical processes related to sediment resuspension and river inflows may obscure the local effects of *Dreissena*. Identifying and modeling factors that impact water quality spatially and temporally is crucial for separating *Dreissena* effects from background variability.

Time series advanced very high resolution radiometer (AVHRR) R_{rs} imagery is applied to the study of water quality in Saginaw Bay, Lake Huron, over a 7-yr period from 1987 to 1993. Shipboard sampling data, provided by the NOAA Great Lakes Environmental Research Laboratory (NOAA/GLERL), are used in the comparison of in situ water quality variables to satellite-derived reflectances. Visual analysis of the spatial images, as well as point data corresponding to NOAA/GLERL sampling stations, provides insights into the magnitude of spatial and temporal changes brought about by the zebra mussel.

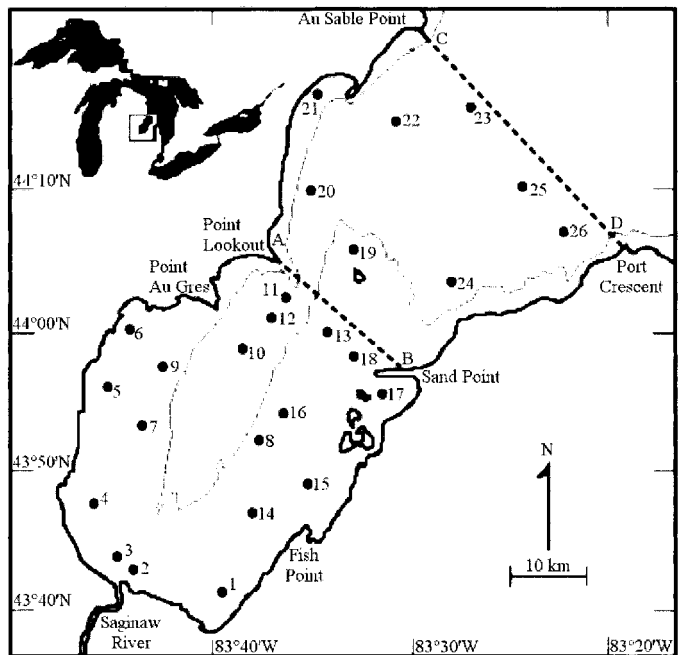


Fig. 1. Location map of Saginaw Bay, Lake Huron. Line AB between Point Lookout and Sand Point divides the inner and outer bay, and line CD between Au Sable point and Port Crescent divides the outer bay and Lake Huron. The 8 m bathocline is also shown. NOAA/GLERL sampling locations are numbered 1–26.

Saginaw Bay ecosystem

Saginaw Bay is a large embayment that discharges into Lake Huron, through a mouth 42 km wide between Point Aux Barques to the south and Au Sable Point to the north. The axis of the embayment extends 82 km southwest to the mouth of the Saginaw River (Fig. 1). Based on depth and morphometry differences, Saginaw Bay can be subdivided further into an inner and an outer bay region, the boundary of which is marked by a narrow constriction (21 km) from Point Lookout to Sand Point. A broad shoal from Charity Island to Sand Point increases the distinction between the two bay portions.

Although the surface areas of the two regions are roughly comparable, the inner bay is quite shallow, with a mean depth of 4.6 m compared to the outer bay's mean depth of 15 m. Because of its shallow depth, the water volume of the inner bay constitutes only 30% of the bay's total water volume, whereas the outer bay comprises 70%. A narrow and relatively deep channel (8 m) extends into the inner bay just west of Point Lookout and is flanked on all sides by extensive sandy shallows, prompting a further classification of the bay into central and coastal regions (Freedman 1974).

Water quality in the bay has followed historic patterns common to other freshwater bays in the Great Lakes. In the period before the mid-1970s, there were anthropogenically induced increases in nitrogen and phosphorus concentrations, as well as blooms of noxious bluegreen algae (Freedman 1974). Certain regions of Saginaw Bay had the highest standing stocks of phytoplankton of any area in the Great Lakes (Vollenweider et al. 1974). Following phosphorus

abatement programs in the mid-1970s, water quality improved markedly. Decreased concentrations of phosphorus resulted in reductions in standing stocks of phytoplankton and in Chl *a* concentrations (Bierman et al. 1984). However, seasonally higher concentrations of phosphorus and lower Secchi disc depths (SD) were found in the most highly degraded regions of Saginaw Bay, suggesting that wind-induced sediment resuspension contributed to elevated phosphorus concentrations during spring and fall months (Bierman et al. 1984).

Typical pre-*Dreissena* Secchi depths in Saginaw Bay were in the range of 0.5–2.5 m in the inner bay in 1974–1980 (Nalepa et al. 1996). This compares favorably with average Secchi depths of 0.75–1.6 m prior to the first large recruitment of *Dreissena* in 1991 and to TSS concentrations of 11.6 to 17.0 mg L⁻¹ in the inner bay from samples obtained at 1 m depths from April to November by EPA between 1976–1980 (from EPA STORET: <http://www.epa.gov/OWOW/STORET/>).

Methods

Image processing—The AVHRR imagery was obtained from two sources: the USGS Eros Data Center (EDC) for the 1987 spring 1991 images and the NOAA Coastal Active Access System (NCAAS), an online archiving service provided through NOAA's CoastWatch Program, for the summer 1991–1993 images. Preprocessing of the EDC images corrected for geometric and radiometric anomalies of the data. The images were georegistered to an Albers equal area projection and resampled to a 1 km² pixel size using the nearest neighbor algorithm. Eleven-bit data were converted to 16-bit data and satellite counts were converted to albedos according to Teillet and Holben (1994) and Kidwell (1991). Twelve of the sixteen EDC processed images were from NOAA 9, in which prelaunch calibrations for channels 1–2 degraded significantly over time (Rao et al. 1993; Rao and Chen 1995).

As part of preprocessing, the NCAAS images were georectified to a Mercator projection, converted to albedo in the form $\pi L_*/E_o$, where L_* is total radiance received at the satellite and E_o is the solar constant. The data were subset into 512 × 512 k data sets with a pixel of 1.34 km². DECCON, a freeware program developed for use with the CoastWatch images, was used to strip off header information and to convert the data from 11-bit to 8-bit format for importing into the image-processing software (Townsend and Stumpf 1996). In addition, DECCON converted channels 1 and 2 from albedo to aerosol-corrected reflectance ($R_c[\lambda]$, where λ = wavelength) with the default settings for a range of 0–12.5%.

Image processing was accomplished using IDL/Envi image-processing software. Land values and dense clouds were eliminated in the aerosol correction. R_{rs} was obtained from $R_c(\lambda)$ using the method described in Stumpf and Frayer (1997). A pixel interrogation procedure within IDL/Envi estimated residual bias in the reflectance imagery due to Rayleigh scattering and some residual haze. A region of clear water in the outer bay was identified where Secchi depths

were consistently high (~5–6 m) (Nalepa et al. 1996) and corresponding $R_c(\lambda)$ was consistently low (0.05–0.25%). Reflectances greater than the clear water values were attributed to the atmosphere and subtracted from each image. Therefore, the procedure forced reflectances at the clear water control site to be extremely small, and the subtraction left only the clear water signal. This approach of correcting for the Rayleigh component is analogous to the dark object subtraction used in studies over land. Seventy-two cloud-free AVHRR images spanning spring, summer, and fall months from 1987 to 1993 resulted.

Relationship of water quality variables to reflectance—A relationship between R_{rs} and in situ water quality parameters was established using shipboard sampling data (i.e., total suspended solids and Secchi disc depths) obtained from NOAA/GLERL sampling stations in Saginaw Bay (Fig. 1). The purpose of the comparison was twofold—to provide a physical basis for comparing satellite-derived reflectances to in situ water quality parameters and to provide estimates of suspended solid concentrations and Secchi disc depths from the satellite data. The in situ data covered a 3-yr period from 1991 to 1993. R_{rs} used in the regressions were taken from the median value of a 3 × 3 pixel region at the 26 sampling sites.

Shipboard sampling occurred at monthly intervals at 26 stations from April to November in 1991 and April through October in 1992. In 1993, 13 stations were sampled on seven occasions from April to October. Sites were omitted based on their similarity to adjacent sites using cluster analysis (Johengen et al. 1995). Water clarity was measured by a 20 cm Secchi disc (Fahnenstiel et al. 1995). Total suspended solids (TSS) were determined gravimetrically after Nalepa et al. (1996). Between 500 and 2,000 ml of sample were filtered through a predried, preweighed Whatman GF/C 47-mm filter.

We regressed R_{rs} on inverse SD (m⁻¹) and TSS for data obtained during 1991–1993. We assessed model fit using the coefficient of determination, r^2 , tested the hypothesis that the slope of the regression equation = 0.0, and constructed a 95% confidence interval for the intercept B_0 to assess the bias of the regression equations. Simple linear regressions of reflectance versus inverse SD (m⁻¹) and TSS for 1991–1993 are presented in Fig. 2.

R_{rs} models—In the Great Lakes, retrospective water quality studies have been hampered by the lack of in situ measurements prior to the occurrence of *Dreissena*. One major advantage of remote sensing is the serial nature of the measurements (1–2 band passes per day for AVHRR R_{rs}) during periods when shipboard sampling data are not available. However, the vast amount of synoptic data (e.g., >1,500 data points or pixels per image for the Saginaw Bay water signature only) necessitates reduction of the data, so we subset data from 24 sampling stations established by NOAA/GLERL (Nalepa and Fahnenstiel 1995) in our analysis.

Point data obtained from the mean of a 3 × 3 pixel block located at the NOAA/GLERL sampling locations for each of 24 stations were extracted from the AVHRR images. We used four images in each of 1987 and 1988, three images in

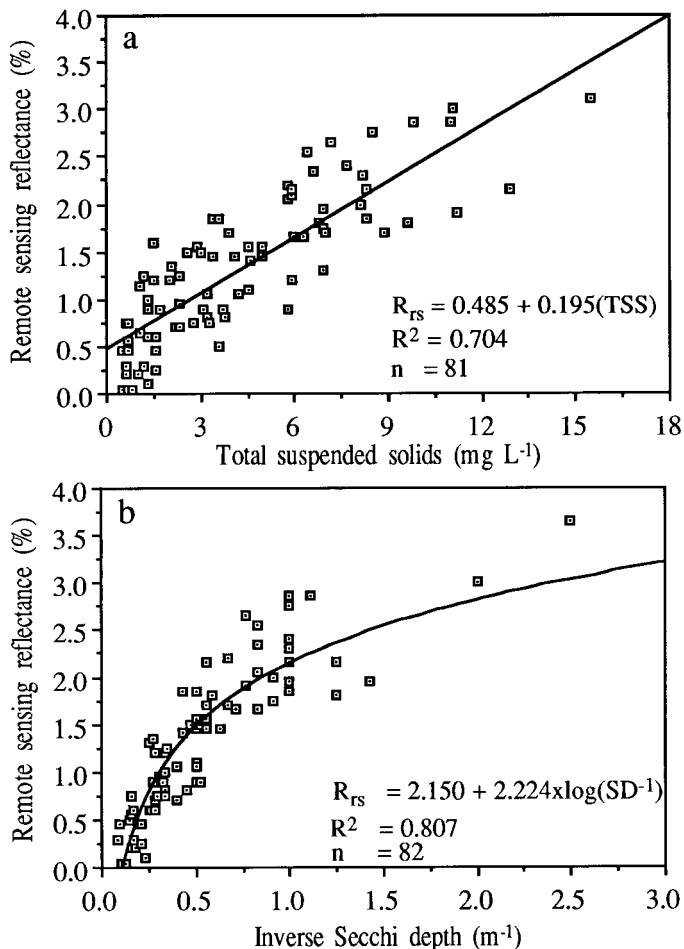


Fig. 2. Simple linear regression results for the comparison of satellite-derived R_{rs} to (a) total suspended solids and (b) inverse Secchi disc depth.

both 1989 and 1990, and 18, 26, and 16 images in 1991, 1992, and 1993, respectively. We classified each site for each year as having high, low, and zero zebra mussel density following Fahnenstiel et al. (1995). High density was defined as $>4,000$ individuals m^{-2} . Six inner bay sites (Stas. 5, 6, and 13–16), and one outer bay site (Sta. 19) were classified as high-density sites for 1992–1993. Twelve inner bay sites (Stas. 1–4, 7–12, 17 and 18) experienced low zebra mussel densities ($<4,000$ individuals m^{-2}) in 1992–1993. Outer bay Stas. 21–23 and 25–26 had zero zebra mussel density over the course of the entire study.

Estimation of changes in R_{rs} associated with *Dreissena* presence is complicated by the lack of temporal balance in the available image data. The possibility of variation in R_{rs} over the course of the summer within a year (seasonal effects) precludes simple averaging of R_{rs} levels within a year and subsequent comparison of annual means. The available images also suggested significant variation between sites that needs to be accounted for. To estimate *Dreissena* effects, we built a regression model for R_{rs} that incorporates seasonal and site effects, as well as possible *Dreissena* effects.

We determined that the model should include three main effects: (1) a site effect (SITE) that captures reflectance level

variation by site, perhaps due to variation in bathymetry, proximity to discharge, or degree of mixing at or near a site; (2) a seasonal effect captured by polynomial terms in day of year (DAY), for nearly all sites R_{rs} tended to be higher in early and late summer, so we modeled the seasonal effect as a second-order polynomial in day; (3) a *Dreissena* density class effect (CLASS), the effect of greatest interest, which measures the impact of a particular level of *Dreissena* density at zero-, low-, or high-density sites on R_{rs} .

Given the variation in site characteristics, we suspected that *Dreissena* effects on R_{rs} could vary across sites and that two sites with similar *Dreissena* density levels could experience different magnitudes of effect on R_{rs} . We allowed for the possibility by including a site by density class interaction term (site \times class). Similarly, seasonal patterns could vary by both site and by density class so we initially included interaction terms between density class and day of year (class \times day) and between site and day of year (site \times day).

We pooled data across all sites and years (total $n = 1,728$) and fit the regression model:

$$\begin{aligned}
 R_{rs} = & B_0 + B_{1i} \cdot \text{SITE}_i + B_{2j} \cdot \text{CLASS}_j + B_3 \cdot \text{DAY} \\
 & + B_4 \cdot \text{DAY}^2 + B_{5ij} \cdot \text{SITE}_i \cdot \text{CLASS}_j \\
 & + B_{6i} \cdot \text{SITE}_i \cdot \text{DAY} + B_{7i} \cdot \text{SITE}_i \cdot \text{DAY}^2 \\
 & + B_{8j} \cdot \text{CLASS}_j \cdot \text{DAY} + B_{9j} \cdot \text{CLASS}_j \cdot \text{DAY}^2
 \end{aligned}$$

for $i = 1, 2, \dots, 24$ sites;
 $j = 1, 2, 3$ *Dreissena* density classes.

R_{rs} denotes the reflectance at a particular site on a particular day of year; B_0 denotes a constant term; B_{1i} is a site-specific constant; B_{2j} is the effect of the j th level of *Dreissena* density, the effect of greatest interest; B_3 and B_4 are regression coefficients for the linear and quadratic terms in day of year; B_{5ij} is the effect of density class j at site i ; B_{6i} and B_{7i} are the site-specific coefficients of day and day²—these terms allow the seasonal component to vary by site; B_{8j} and B_{9j} are the density class specific coefficients of day and day²—these terms allow the seasonal effects to vary by *Dreissena* density class.

This model is extremely complex with many parameters, so we simplified it by eliminating terms that did not contribute significantly. We selected a model based on the adjusted coefficient of determination, R_A^2 , and the Akaike information criteria (AIC). These measures compare the fit between competing models and compensate for the number of model parameters, which the coefficient of determination R^2 does not (Rawlings et al. 1998). We assessed the predictive ability of competing models by summing the squared values of the Press residuals, which are the prediction error at a given data point if that data point was not included in the parameter estimation (Rawlings et al. 1998). Using these three criteria, the best model is that which has the largest R_A^2 , the smallest AIC, and the smallest Press statistic, although there is no guarantee that these criteria result in the selection of the same model. We fit the model using SAS PROC GLM (SAS Institute 1996) and eliminated model terms using backward elimination. We kept only those fac-

tors that were significant at the $\alpha = 0.05$ level based on the SAS TYPE III sums of squares and computed AIC, R_A^2 and the Press statistic for each resulting model. Final model fit was assessed using site-specific plots of predicted and observed reflectance values over time.

Prediction of TSS—We used the resulting R_{rs} model to predict R_{rs} at each site for those days on which TSS data were available. We converted the predicted R_{rs} into predicted TSS using the linear regression equation relating R_{rs} and TSS derived from the shipboard data. The algorithm has three steps: (1) Determine a calibrating equation relating R_{rs} to TSS from shipboard data: $R_{rs} = a + b(\text{TSS})$. This yields the inverse, or calibrating equation, $\text{TSS} = (R_{rs} - a)/b$. (2) Use the spatial-temporal model for R_{rs} from image-derived reflectance data to predict R_{rs} at sites and dates when TSS data are available. (3) Insert these predicted values of R_{rs} into the calibrating equation $\text{TSS} = (R_{rs} - a)/b$ to obtain predicted TSS. We assessed the prediction error by constructing site-specific plots of observed and predicted TSS over time and decomposed the mean squared prediction error into a bias and variance component (Rawlings et al. 1998). A low percent bias is desirable.

Results

Relationship of AVHRR R_{rs} to in situ water quality variables—Simple linear regressions of the CoastWatch (NOAA 11) data against the water quality parameters for 1991–1993 indicate a strong linear association within the range of conditions sampled in Saginaw Bay (Fig. 2a,b). The models, $R_{rs} = 0.485 + 0.195(\text{TSS})$ and $R_{rs} = 2.150 + 2.224 \times \log(\text{SD}^{-1})$, account for 70 and 81% of the total variance in the in situ data (>80 data points). The predicted values of R_{rs} for pure lake water are 0.5% and asymptotic for inverse SD. A 1 mg L⁻¹ increase in total solids yields a 0.2% increase in reflectance.

Shipboard sampling collected during individual years (1991, 1992, and 1993), as well as data collected on 20–21 May 1991 were used to construct similar regressions. The May 1991 data were used with an EDC-supplied image acquired on 19 May 1991, although fewer numbers of data points ($n = 10$) were used in the analysis. The coefficients of determination (r^2) for the regressions of R_{rs} versus the in situ water quality parameters exceeded 0.70 for 1991 and 1993 (r^2 range = 0.70–0.89), but were below 0.70 in 1992 ($r^2 = 0.62$) and on 19 May 1991 ($r^2 = 0.68$) for the comparison of TSS to R_{rs} . Atmospheric anomalies due to haze or pollution not removed in the clear water subtraction or inaccuracies in the cloud discrimination procedure may account for the discrepancy in 1992, whereas time of acquisition of shipboard sampling data versus satellite overpass may explain the relatively poorer fit of the EDC data. R^2 values in the comparison of reflectance to inverse SD are consistently higher.

The expected value of R_{rs} at the intercept, that is, for pure water, is zero; however, some reflectance is found in open lake waters due to autochthonous production. The 95% confidence interval of the intercept for the 1991–1993 regression model is $0.49 \pm 0.15\%$ R_{rs} , which indicates some bias in the

intercept. Overall, the models tended to overestimate B_0 by 0.1 to 0.5% R_{rs} .

Satellite imagery: Pre-Dreissena seston concentrations—The spatial distribution of suspended materials in the pre-Dreissena images (1987–summer 1991) was distinctly different during spring, summer, and fall months. These differences in suspended solids were indicated by peaks in satellite-derived R_{rs} , corresponding to different regions of the inner and outer bay. For example, the dominant feature during spring months was the Saginaw River discharge, observed in multiple images (e.g., 7 May 1987, 8 May 1987, 18 May 1988, 31 May 1990, and 19 May 1991; example shown in Fig. 3a and scatter plots from selected sampling stations shown in Fig. 4). The Saginaw River plume corresponds to a large sediment deposition zone (mapped by Robbins 1986) in the central bay covering approximately 400 km² and is the dominant feature during spring. In Fig. 3a the plume projects into both the central and eastern portion of the inner bay, a distance of 75 km from the mouth. Point data from the sampling stations reveal that sites 4, 7, 9–12 were most heavily affected by the plume (e.g., Fig. 4c, Sta. 7).

The spatial distribution of suspended solid concentrations was reversed in summer months, when the highly productive near-shore regions of the inner bay experienced higher turbidity (plankton) than the central inner bay (Fig. 3d,g). Reflectances in the central inner bay were generally lower ($R_{rs} = 1$ –2%, $\text{TSS} = 2.6$ –7.8 mg L⁻¹), whereas reflectances in the near-shore regions (Point Au Gres to the mouth of the Saginaw River and north to Sand Point and Charity Island) were elevated ($R_{rs} = 2.5$ –3.5%, $\text{TSS} = 10.3$ –15.5 mg L⁻¹). In fall, wind-driven resuspension increased inner bay reflectances, particularly in the productive southeastern portion of the inner bay (Fig. 3j).

Different physical processes influence measures of water quality in the inner and outer bay, resulting in inherently different characteristics between these zones. Seasonally, runoff and inputs from the Saginaw River in spring, uptake of nutrients and growth of phytoplankton in summer, and resuspension events in fall account for high turbidity in the inner bay. In contrast, the combination of deeper bathymetry and dominance of less turbid Lake Huron water driven by near-shore currents affords opportunities for water mass exchange, mixing, and dilution of outer Saginaw Bay. This accounts for overall lower reflectances and less variability of suspended sediment concentrations in the outer bay on a seasonal basis (Fig. 3d). One notable exception was found in the south central outer bay at Charity Island, where reflectances were consistently higher in summer due mostly to biological production (Fig. 3g,j).

Post-Dreissena seston concentrations—Satellite images from 1992–1993 (post-Dreissena) contrast with the pre-invasion images. Whereas the Saginaw River plume was the dominant feature in the pre-Dreissena images, seston concentrations were greatly reduced in all of the post-Dreissena imagery (Fig. 3b,c, 3e,f, 3h,i, 3k,l). Evidence that suspended sediment concentrations were lower in 1992 and 1993 is found by visual review of the reflectance maps, point data

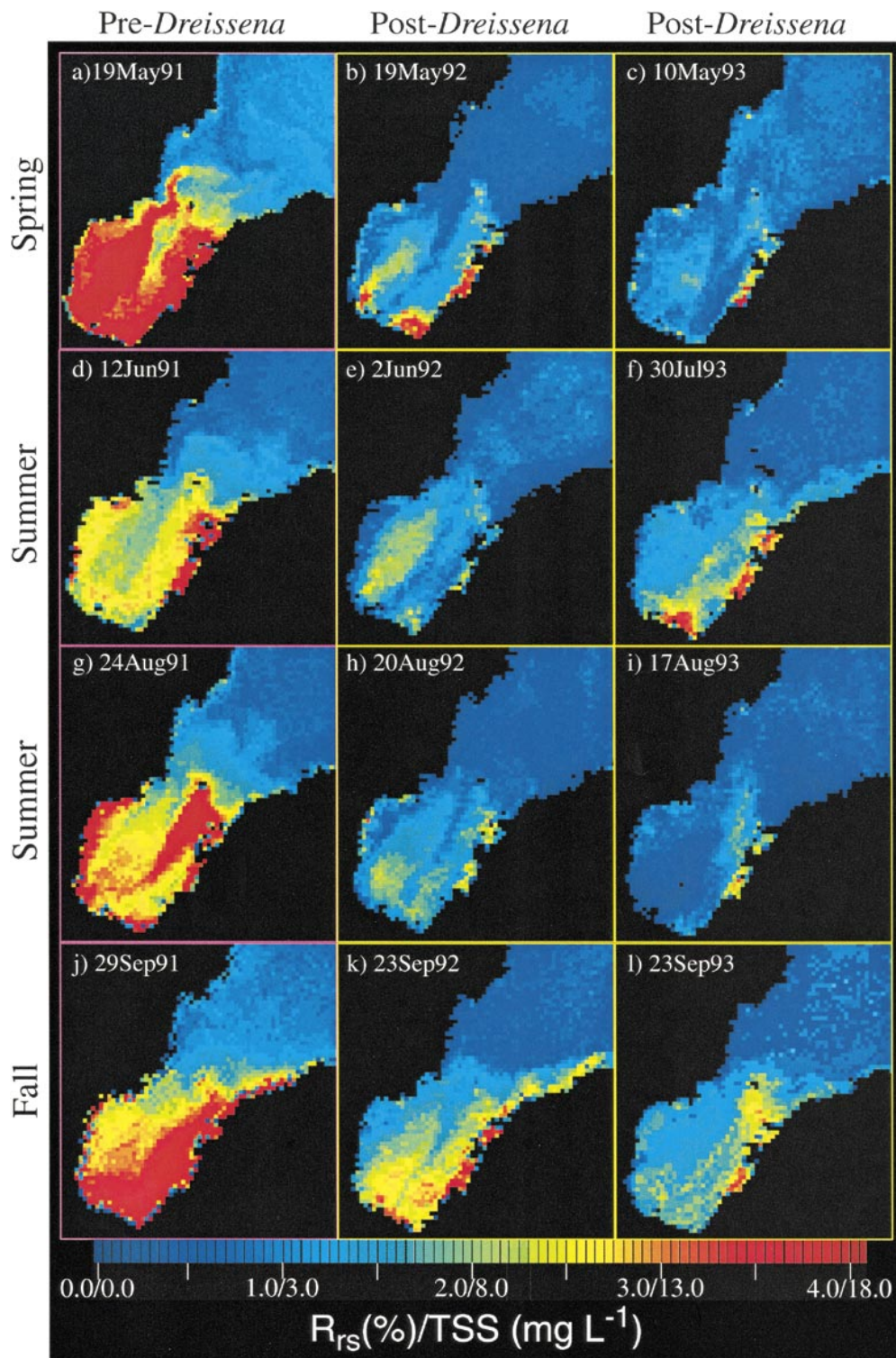


Fig. 3. Time series R_{rs} images of Saginaw Bay for the pre-*Dreissena* (1991) versus post-*Dreissena* period (1992–1993). Seston concentrations were uniformly lower in the post-*Dreissena* years.

from scatter plots (Fig. 4), and in the model results. Suspended sediment concentrations associated with the Saginaw River were greatly reduced in the spring images from 1992 and 1993 (Fig. 3b,c). Comparison of point data from imagery collected 1 yr apart on 19 May 1991, 19 May 1992, and

10 May 1993 that corresponded to river plume Stas. 4, 7, and 9 indicated a 41–52% decrease in reflectances from 1991 compared to 1992 and 1993.

Summer reflectances in the pre-*Dreissena* images were much higher in the productive shallows and lower in the

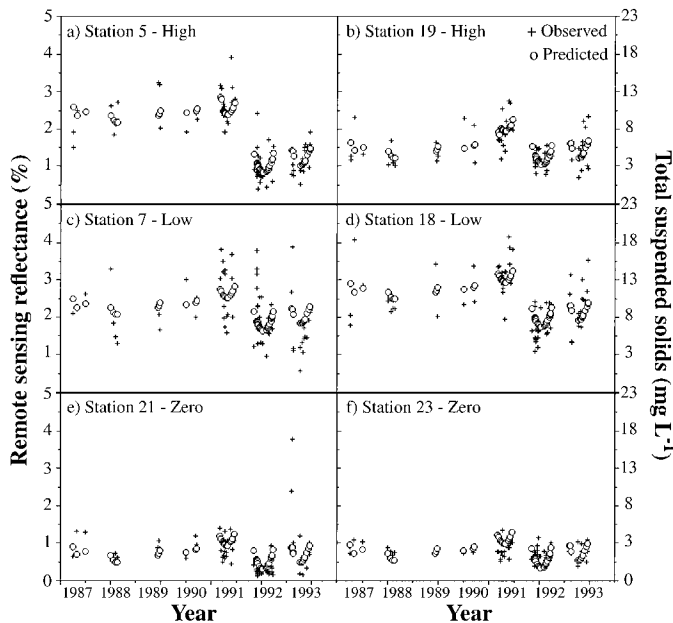


Fig. 4. Observed vs. predicted R_{rs} for Saginaw Bay for selected sampling stations. (a),(b) High-density sites 5 (inner bay) and 19 (outer bay); (c),(d) low-density sites 7 (inner bay river plume) and 18 (inner bay coastal shallows); and zero-density sites 21 (near-shore outer bay) and 23 (offshore outer bay). The results of the linear regression of R_{rs} and TSS are used to provide estimates of changes in total suspended solids.

central deposition zone, whereas the post-*Dreissena* images showed the opposite trend regardless of season. For example, sites with high densities of zebra mussels (Stas. 5–6 and 13–16) had reflectances in the range expected for the relatively nonturbid outer Saginaw Bay during summer months (approximately 0.5–1.0% or 0.1–2.5 mg L⁻¹ TSS), whereas reflectances in the central inner bay remained relatively unchanged. Exceptions included late July 1993 at locations in the far southeastern portion of the bay (Stas. 1, 2), near Sebewaing (Sta. 15), and near Bay Port (Sta. 17), where reflectances were elevated to pre-*Dreissena* levels (Fig. 3f). The localized high turbidity likely corresponded to blooms of the highly reflective cyanobacteria *Microcystis*, which was observed at several sampling locations in late summer 1993, as well as in subsequent years (Nalepa and Fahnenstiel 1995).

Post-*Dreissena* images obtained during fall months were most similar to the pre-*Dreissena* images, due to wind-driven resuspension of sediments, although reflectances were lower overall. (Fig. 3k,l). High-density sites (Stas. 5–6, 13–16, and 19) showed persistent low R_{rs} of the range 0.50–1.00% (of the same magnitude as open Lake Huron waters) regardless of season (Fig. 3b,c vs. Fig. 3i,j and Fig. 3k,l) indicating the most severe effects; however, reflectances throughout the inner bay were lower after zebra mussels were established, indicating basin-wide effects.

R_{rs} models—Plots of R_{rs} over time (Fig. 4) indicated that reflectances were greater at all inner bay sites from 1987 to 1991 compared to 1992–1993, with lowest average R_{rs} in

1992 (11 of 18 inner bay stations). Most marked decreases were observed at sites with high zebra mussel densities (Stas. 5–6, 13–16). Moderately impacted Stas. 1, 3, 7, 9, and 14 (marginal) showed lower annual reflectances during 1992 compared to 1993. Outer bay sites had uniformly lower reflectances of approximately 0.5–1.0% (TSS = 1.3–2.6 mg L⁻¹). These stations also had lower reflectances during 1992 compared to 1993 (seven of eight stations), and six of eight outer bay stations had the lowest average reflectances over the seven year period during 1992.

All three model selection criteria, R^2 , AIC, and minimum prediction error, yielded the same model:

$$R_{rs} = B_0 + B_{1i} \cdot \text{SITE}_i + B_{2j} \cdot \text{CLASS}_j + B_3 \cdot \text{DAY} \\ + B_4 \cdot \text{DAY}^2 + B_{5ij} \cdot \text{SITE}_i \cdot \text{CLASS}_j \\ + B_{6i} \cdot \text{SITE}_i \cdot \text{DAY} + B_{8j} \cdot \text{CLASS}_j \cdot \text{DAY}$$

$$R^2 = 67.4\%; \quad R_A^2 = 65.9\%$$

for $i = 1, 2, \dots, 24$ stations and

$j = 1, 2, 3$ *Dreissena* density classes.

The analysis indicates that R_{rs} varies significantly by site ($P = 0.0001$), *Dreissena* density class ($P = 0.0001$), and by day of year in a nonlinear pattern (day, $P = 0.1749$, day², $P = 0.001$). The effect of *Dreissena* colonization varied by site as evidenced by the significance of the site \times class interaction ($P = 0.0001$). Seasonal patterns also varied by site (site \times day, $P = 0.0001$) and by density class (class \times day, $P = 0.0167$).

Plots of observed and predicted R_{rs} over time indicate that the model captures the seasonal and interannual variability in the concentrations of suspended solids in the bay (Fig. 4). Trends in observed and predicted values of reflectances follow similar patterns at each station—highest values are found during 1991 and lowest during 1992 at all stations, with slightly higher R_{rs} in 1993 compared to 1992. The model reasonably predicts R_{rs} except in the case of Stas. 21, 22, 23, 25, and 26, which were all classified as zero-density sites, with systematic overprediction of reflectance values in 1992–1993. The implication is that even the no impact sites experienced some decrease in reflectance. Outer bay stations exhibit the same patterns during the pre- versus post-*Dreissena* periods; however, the decrease in reflectance is much less marked at outer bay stations compared to inner bay stations.

The R_{rs} model indicated that the effect of *Dreissena* presence on R_{rs} varied by site and day of year, necessitating a site by site and day by day interpretation of the model parameters. Using the model, we estimated R_{rs} levels for pre- (1987–1991) and post- (1992–1993) *Dreissena* invasion for each site on each of three dates (19 May, 19 June, and 19 September) and calculated the change in R_{rs} from these estimates (Table 1). We then used the regression equation relating R_{rs} to TSS to calculate estimated changes in TSS. The three dates represent early, middle, and late summer dates that fall within the temporal range of the available data, although other dates could be used.

The largest estimated decreases in R_{rs} (and TSS) occurred

Table 1. Model-based estimates of reflectance decrease for low and high impact sites on 19 May, 19 July, and 19 September. Estimated changes in total suspended solids (mg L^{-1}) are given in parentheses.

Site	Estimated percent decrease		
	May	Jul	Sep
Low impact sites			
1	1.27 (6.51)	1.16 (5.95)	1.04 (5.33)
2	1.16 (5.95)	1.05 (5.38)	0.94 (4.82)
3	1.14 (5.85)	1.03 (5.28)	0.92 (4.72)
4	0.94 (4.82)	0.83 (4.26)	0.72 (3.69)
7	0.73 (3.74)	0.62 (3.18)	0.51 (2.62)
8	1.08 (5.54)	0.97 (4.97)	0.86 (4.41)
9	0.81 (4.15)	0.70 (3.59)	0.59 (3.03)
10	0.90 (4.62)	0.79 (4.05)	0.67 (3.44)
11	0.87 (4.46)	0.75 (3.85)	0.64 (3.28)
12	1.00 (5.13)	0.88 (4.51)	0.77 (3.95)
17	1.28 (6.56)	1.17 (6.00)	1.06 (5.44)
18	1.10 (5.64)	1.00 (5.13)	0.88 (4.51)
High impact sites			
5	1.45 (7.44)	1.43 (7.33)	1.41 (7.23)
6	1.38 (7.08)	1.36 (4.49)	1.34 (6.87)
13	0.42 (2.15)	0.40 (2.05)	0.39 (2.00)
14	1.16 (5.95)	1.14 (5.84)	1.12 (5.74)
15	0.77 (3.95)	0.76 (3.90)	0.74 (3.79)
16	0.73 (3.74)	0.71 (3.64)	0.70 (3.59)
19	0.23 (1.18)	0.22 (1.13)	0.20 (1.03)

during spring for all sites, and overall at sites with high *Dreissena* density (i.e., Stas. 5–6, 13–16, 19). Estimated decreases in R_{rs} at low-impact sites ranged from 0.73 to 1.28% (3.74–6.56 mg L^{-1} TSS) (Table 1). High-density sites 5 and 6 had the greatest estimated decreases, 1.45% (7.44 mg L^{-1} TSS) and 1.38% (7.08 mg L^{-1} TSS), respectively. We note that Stas. 13, 16, and 19 were all classified as high-impact sites, but in some cases had estimated impacts lower than those of low-density sites. To further illustrate, we estimated midsummer (19 July) year specific R_{rs} levels for low, moderate, and high-impact sites (Fig. 5). High-density classes

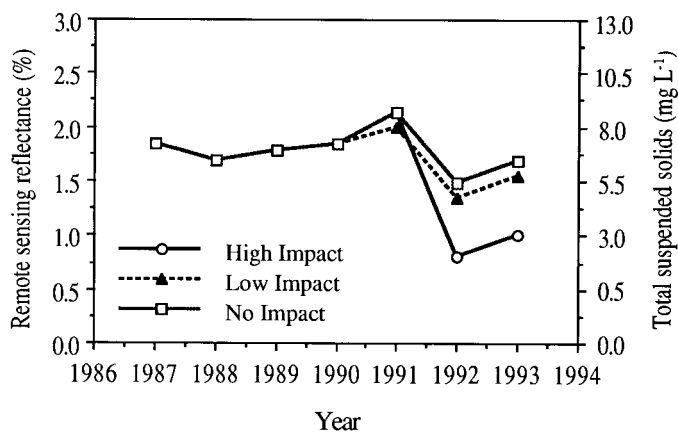


Fig. 5. Model-based changes in reflectance for average high-, low-, and no-density stations by year during midsummer (day of year = 200 or July 19).

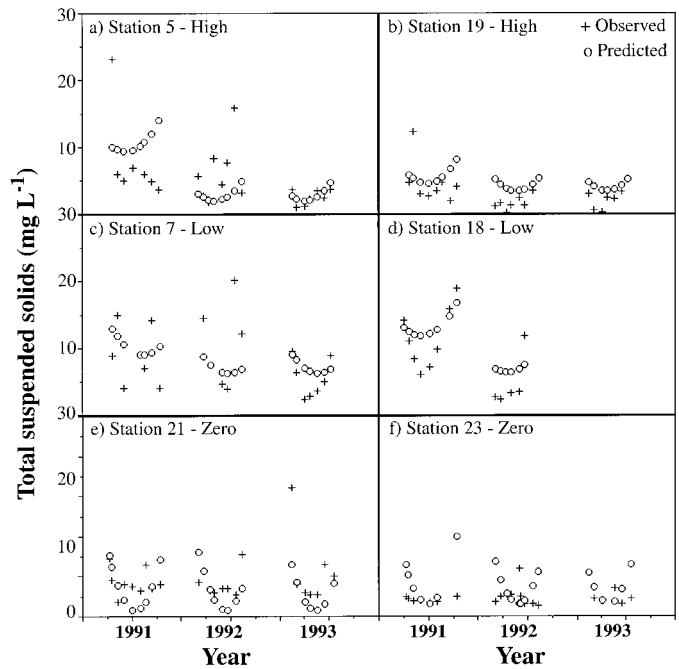


Fig. 6. Observed versus predicted TSS for selected sampling locations in Saginaw Bay. (a),(b) high-density sites 5 (inner bay) and 19 (outer bay), (c),(d) low-density sites 7 (inner bay, river plume) and 18 (inner bay coastal shallows; note that in 1993 in situ TSS samples were not taken at Sta. 18), and zero-density sites 21 (near-shore outer bay) and 23 (offshore outer bay).

Table 2. Mean square error and percentage bias for predicted values of TSS for sampling dates in 1991–1993.

Site	N	MSEP	% bias
1	14	108.264	14.4844
2	11	30.060	0.1945
3	13	44.750	4.1059
4	18	30.142	0.1464
5	22	28.870	0.1403
6	14	52.684	3.7221
7	18	24.869	0.0267
8	13	19.076	46.0331
9	13	24.098	1.3993
10	21	18.254	8.4723
11	24	21.123	1.5524
12	12	9.783	47.7705
13	22	12.564	38.4456
14	17	30.222	6.8700
15	13	35.280	21.5946
16	19	16.314	4.8584
17	13	14.707	21.8138
18	13	12.262	29.1851
19	21	8.687	38.0339
21	23	1.591	19.1920
22	16	1.418	43.6770
23	22	1.344	22.6533
25	15	1.771	68.7795
26	17	2.010	36.1892

experienced the greatest decrease, although zero impact sites also experienced decreases in R_{rs} .

TSS prediction—Observed and predicted values of TSS for sampling dates in 1991–1993 (Fig. 6 for selected stations) indicate that although predicted values of TSS are reasonable, there is a tendency for systematic overprediction in some sites. The bias component of the mean squared error of the prediction errors ranged from <1.0% to 68.7% with strong evidence of bias at most outer bay sites, as well as Stas. 8, 12, 13, and 15 (percentage bias > 20%) (Table 2). The reflectance model tended to overpredict R_{rs} at outer bay sites, which would in turn lead to overprediction of TSS. Plots of predicted error versus TSS indicated that the magnitude of the errors increased with increased TSS. The model works best at low TSS concentrations (<10 mg L⁻¹) but performs poorly above that level, implying that performance is best during midsummer when lowest TSS values tend to occur.

Discussion

The satellite-derived seston maps and model output highlight temporal and spatial changes in suspended solids concentrations in Saginaw Bay as related to inputs from the Saginaw River and Lake Huron water mass circulation (morphometry). These results illustrate typical seasonal and interannual turbidity patterns prior to the establishment of zebra mussels in Saginaw Bay, at a time when shipboard monitoring was not conducted. The pre-*Dreissena* imagery illustrates that the inner bay's major source of suspended material is the Saginaw River, which is dominant in the spring, whereas the outer bay is more clearly dominated by open Lake Huron waters (Bierman et al. 1984). Water clarity in the deep northwestern outer Saginaw Bay is controlled by Lake Huron near-shore currents (Danek and Saylor 1975; Budd et al. 1998), whereas the shallow southeastern outer bay is more subject to the water mass transport from productive inner bay waters.

In combination with the intensive, multiyear in situ sampling program, the R_{rs} maps and regression models provide detailed information about basin-wide changes in water clarity brought about by the zebra mussel. Seston concentrations are consistently lower regardless of season after zebra mussels were established in the bay. Moreover, the surface spatial distribution of suspended materials is more similar for all seasons during the post-*Dreissena* years, particularly at high-density sites.

Water mass circulation and morphometry differences, as well as the location of suitable substrates, contributed to the spatial variability of zebra mussel colonization in Saginaw Bay. These changes correspond to the monitored spatial distributions of *Dreissena* populations from 1990 to 1993 (Nalepa et al. 1995). For example, zebra mussel densities were low at river plume Stas. 4 and 7 (no data for Sta. 9) characteristic of inner bay sites with soft substrates, whereas planktonic zebra mussel larval densities tended to be higher at these same two stations (Nalepa et al. 1995). Thus, the same current patterns that tend to focus suspended particulates (Robbins 1986) may transport plankton to these re-

gions. Alternatively, predation by adult zebra mussels (MacIsaac et al. 1991) may also account for the lower veliger densities found at highly impacted sites (Nalepa et al. 1995).

There were some surprises in the spatial data and linear models, which may be explained by changes in zebra mussel densities at highly impacted sites from 1991 to 1993. Systematic overprediction of TSS from highly impacted Sites 13–16 may be related to the local population dynamics. For example, Sta. 15 had very high recruitment of postveliger larvae in the fall of 1991 (43,000 ind. m⁻²); however, zebra mussel densities had plummeted in fall 1992 to 5,500 m⁻² and leveled off in 1993 at 7,341 m⁻² (Nalepa et al. 1995). Similar declines were observed at Sites 13, 14, and 16 from 1992 to 1993. The anomalously high reflectances observed in the southeastern portion of the inner bay during fall 1992 (Fig. 3k) and late summer 1993 (Fig. 3f) may correspond to cyanophyte blooms in Saginaw Bay (Gardner et al. 1995; Fanslow et al. 1995). Blooms of *Microcystis* were observed again in 1994 in Saginaw Bay and in western Lake Erie during 1995 (Budd et al. in press). The reflectance maps and descriptive models confirm the presence of higher seston densities associated with ship-based observations of *Microcystis* blooms and provide a level of spatial detail that would be difficult to duplicate from shipboard sampling alone.

Dramatic shifts in R_{rs} match changes from the in situ water quality data, particularly at sampling sites with high densities of zebra mussels. For example, shipboard sampling data for total phosphorus and Chl *a* decreased by 66% and 48%, respectively, whereas Secchi visibilities increased 88% at high-density inner bay sites (1990 to 1993 for Chl *a* and 1991 to 1993 for phosphorus and SD) (Fahnenstiel et al. 1995). When all inner bay sites were averaged regardless of zebra mussel classification, overall decreases of 59% and 43% in in situ Chl *a* and total phosphorus were observed, as well as an increase of 60% in Secchi depth. TSS decreased 44% in 1992 and 62% in 1993 at inner bay sites (Johengen et al. 1995). Similar decreases in satellite-derived reflectances were observed in the AVHRR images on a site by site basis.

The model results suggest an overall decrease in reflectances at outer bay control stations in 1992 and to a lesser extent in 1993, suggesting a net decrease in transport of sediment from the inner to outer bay. Johengen et al. (1995) also found significant differences in TSS at outer bay Sites 20 and 24 for 1991 compared to 1992, but not for the 1991/1993 comparison years, whereas no significant differences in TSS were observed at control Stas. 21–23 and 25–26. Significant differences in Secchi depths, Chl *a*, and kPAR were noted at outer bay stations ($P < 0.01$); however, trends were most distinct and consistent at inner bay stations (Fahnenstiel et al. 1995).

Trends in R_{rs} for specific years can be explained by factors operating over longer time scales. For example, lower reflectances during 1988 compared to other pre-*Dreissena* years may have been due to the fact that 1988 was a drought year (Hartmann 1990). Mean annual reflectances during pre-*Dreissena* years 1987–1989 were also lower on average compared to 1990–1991. However, some of the variability may be explained by the degradation of NOAA-9 prelaunch

calibration for AVHRR channels 1–2, which artificially depressed reflectances (Rao et al. 1993; Rao and Chen 1995). Reflectances were consistently lowest in 1992 when zebra mussel biomass and abundance were highest (Nalepa et al. 1995), whereas reflectances rebounded slightly during 1993 after zebra mussel densities declined threefold.

Differences in R_{rs} between 1991 and 1992 are explained in part by seasonal and interannual differences in runoff to the bay. Phosphorus loadings to Saginaw Bay were higher than normal during spring 1991 and 1992 (2,158 and 946 mt, respectively, compared to 512 mt in 1990), causing high Chl *a* concentrations and metaphytonic algal blooms in 1991 (Fahnenstiel et al. 1995). Reflectances were consistently highest over the 7-yr period in 1991 and lowest in 1992. The anomalous finding for 1992 suggests that zebra mussels, which filtered the entire water volume of inner Saginaw Bay in 1.2 d during 1992 (Fanslow et al. 1995), influenced Chl *a* concentrations and water clarity despite higher than average phosphorus loadings. Review of the 1987–1990 period also suggests that reflectances were significantly lower during the post-*Dreissena* period compared to the pre-*Dreissena* period, although trends were more varied on a site by site basis.

The satellite-derived water quality estimates augment conventional shipboard sampling efforts. Cloud-free satellite images provided synoptic coverage of the entire bay (1649 pixels or samples representing 2,010 square kilometers) on a total of 72 d over the 7-yr period. In situ data were collected less frequently and at fewer stations per day of sampling. For example, shipboard sampling occurred at 26 stations on nine and eight occasions in 1991 and 1992, respectively, and at 13 stations on seven occasions in 1993. Moreover, the satellite images represent some of the only water quality information available for Saginaw Bay from the pre-*Dreissena* period, 1987–1990, although the number of images is limited. Whereas the shipboard sampling program provided detailed information about a broad range of water quality parameters at a given site, the satellite-derived turbidity maps resolve fine scale spatial patterns throughout the bay and highlight specific hot spots where zebra mussel activity is particularly severe.

This research exploits a rich historical archive of AVHRR imagery to “hindcast” the magnitude of biotic effects associated with the introduction and subsequent colonization of *Dreissena* in the Great Lakes. Unfortunately, the CZCS (coastal zone color scanner), which was operational from 1978–1986, was designed for use in the open ocean, so quantitative estimates of sediments or pigments for the highly productive near-shore regions of the Great Lakes was not possible. Now, a new generation of satellite ocean color instruments (e.g., SeaWiFS, Sea-viewing Wide Field-of-view Sensor, and MODIS, moderate resolution imaging spectroradiometer) is available that will greatly improve our ability to monitor and model biotic effects from a variety of causes, including exotic species, harmful algal blooms, and episodic upwelling and resuspension events. Ultimately, we can envision a satellite-based program that monitors, models, and predicts biotic conditions (e.g., *Dreissena* induced *Microcystis* blooms), thereby devising an early warning system for events. The historical AVHRR imagery provides an impor-

tant test of techniques for future application with ocean color instruments.

References

- BIERMAN, V. J., JR., D. M. DOLAN, R. KASPRZYK, AND J. L. CLARK. 1984. Retrospective analysis of the response of Saginaw Bay, Lake Huron, to reductions in phosphorus loadings. *Environ. Sci. Technol.* **18**: 23–31.
- BUDD, J. W., A. M. BEETON, R. P. STUMPF, D. A. CULVER, AND W. C. KERFOOT. In Press. Satellite observations of *Microcystis* blooms in western Lake Erie. *International Association of Theoretical and Applied Limnology: Proceedings of the 27th Congress*.
- , W. C. KERFOOT, AND A. L. MACLEAN. 1998. Documenting complex surface temperature patterns from Advanced Very High Resolution Radiometer (AVHRR) imagery of Saginaw Bay, Lake Huron. *J. Gt. Lakes Res.* **24**: 582–94.
- , ———, A. N. PILANT, AND L. M. JIPPING. 1999. The Keeweenaw current and ice rafting: Use of satellite imagery to investigate copper-rich particle dispersal. *J. Gt. Lakes Res.* **25**:
- DANEK, L. J., AND J. H. SAYLOR. 1975. Saginaw Bay water circulation. NOAA Technical Report ERL 359-GLERL 6, U.S. Department of Commerce.
- FAHNENSTIEL, G. L., G. A. LANG, T. F. NALEPA, AND T. H. JOHNGEN. 1995. Effects of zebra mussel (*Dreissena polymorpha*) colonization on water quality parameters in Saginaw Bay, Lake Huron. *J. Gt. Lakes Res.* **21**: 435–448.
- FANSLAW, D. L., T. F. NALEPA, AND G. A. LANG. 1995. Filtration rate of the zebra mussel (*Dreissena polymorpha*) on natural seston from Saginaw Bay, Lake Huron. *J. Gt. Lakes Res.* **21**: 517–528.
- FREEDMAN, P. L. 1974. Saginaw Bay: An evaluation of existing and historical conditions. Great Lakes Resource Management Program, University of Michigan, Great Lakes Initiative Contract Program Report Number: EPA-905/9-74-003.
- GARDNER, W. S., J. F. CAVALETTI, T. H. JOHNGEN, J. R. JOHNSON, R. T. HEATH, AND J. B. COTNER, JR. 1995. Effects of the zebra mussel, (*Dreissena polymorpha*), on community nitrogen dynamics in Saginaw Bay, Lake Huron. *J. Gt. Lakes Res.* **21**: 529–544.
- HARTMANN, H. C. 1990. Climate change impacts on Laurentian Great Lakes levels. *Clim. Chang.* **17**: 49–67.
- JOHNGEN, T. H., T. F. NALEPA, G. L. FAHNENSTIEL, AND G. GOUDY. 1995. Nutrient changes in Saginaw Bay, Lake Huron, after the establishment of the zebra mussel (*Dreissena polymorpha*). *J. Gt. Lakes Res.* **21**: 465–475.
- KIDWELL, K. B., ED. 1991. NOAA Polar orbiter data user's guide. National Oceanic and Atmospheric Administration.
- LESHKEVICH, G. A., D. J. SCHWAB, AND G. C. MUHR. 1993. Satellite environmental monitoring of the Great Lakes: A review of NOAA's Great Lakes CoastWatch program. *Photogramm. Eng. Remote Sens.* **59**: 371–380.
- MACISAAC, H. J., W. G. SPRULES, AND J. H. LEACH. 1991. Ingestion of small-bodied zooplankton by zebra mussels: Can cannibalism on larvae influence population dynamics? *Can. J. Fish. Aquat. Sci.* **48**: 2151–2160.
- MCMILLAN, L. M., AND D. D. CROSBY. 1984. Theory and validation of the multiple window sea surface temperature technique. *J. Geophys. Res.* **89**: 3655–3661.
- NALEPA, T. F., AND G. L. FAHNENSTIEL. 1995. *Dreissena polymorpha* in the Saginaw Bay, Lake Huron ecosystem: Overview and perspective. *J. Gt. Lakes Res.* **21**: 411–416.
- , ———, M. J. MCCORMICK, T. H. JOHNGEN, G. A. LANG, J. F. CAVALETTI, AND G. GOUDY. 1996. Physical and chemical

- variables of Saginaw Bay, Lake Huron in 1991–1993. NOAA Tech. Memo ERL GLERL-91.
- , J. A. WOJCIK, D. L. FANSLAW, AND G. A. LANG. 1995. Initial colonization of the zebra mussel (*Dreissena polymorpha*) in Saginaw Bay, Lake Huron: Population recruitment, density, and size structure. *J. Gt. Lakes Res.* **21**: 417–434.
- RAO, C. R. N., AND J. CHEN. 1995. Inter-satellite calibration linkages for the visible and near-infrared channel of the Advanced Very High Resolution Radiometer on the NOAA-7, -9, -11 spacecraft. *Int. J. Remote Sens.* **16**: 1931–1942.
- , F. W. STAYLOR, P. ABEL, Y. J. KAUFMAN, E. VERMOTE, W. R. ROSSOW, AND C. BREST. 1993. Degradation of the visible and near infrared channels of the Advanced Very High Resolution Radiometer on the NOAA-9 spacecraft: Assessment and recommendations for corrections. NOAA Technical Report NESDIS 70, Department of Commerce.
- RAWLINGS, J. O., S. G. PANTULA, AND D. A. DICKEY. 1998. Applied regression analysis. Springer.
- ROBBINS, J. A. 1986. Sediments of Saginaw Bay, Lake Huron: Elemental composition and accumulation rates. Special Report No. 102. Great Lakes Research Division, University of Michigan.
- SAS INSTITUTE INC. 1996. SAS/STAT software changes and enhancements. through Release 6.11. SAS Institute.
- STUMPF, R. P. 1995. Retrospective and future studies of coastal water clarity and sediments loads, p. I128–I139. *In Proc. 3rd Thematic Conf. on Rem. Sens. for Marine and Coastal Environ.*
- , AND M. L. FRAYER. 1997. Use of AVHRR imagery to examine long-term trends in water clarity in coastal estuaries: Example in Florida Bay, p. 1–23. *In M. Karhu and C. W. Brown [eds.], Monitoring algal blooms: New techniques for detecting large-scale environmental change.* Landes Bioscience.
- , AND M. A. TYLER. 1988. Satellite detection of bloom and pigment distributions in estuaries. *Remote Sens. Environ.* **24**: 385–404.
- TEILLET, P. M., AND B. N. HOLBEN. 1994. Towards operational radiometric calibration of NOAA AVHRR imagery in the visible and infrared channels. *Can. J. Remote Sens.* **20**: 1–10.
- TOWNSLEY, B., AND R. P. STUMPF. 1996. DECCON software to decompress NOAA IMGMAP compressed imagery and convert to common image file formats. U.S. Geological Survey, Center for Coastal Geology.
- VOLLENWEIDER, R. A., M. MUNAWAR, AND P. STADELMAN. 1974. A comparative review of phytoplankton and primary production in the Laurentian Great Lakes. *J. Fish. Res. Board. Can.* **31**: 739–762.

Received: 7 March 2000

Amended: 11 September 2000

Accepted: 30 October 2000